NEURORADIOLOGY

Iran J Radiol. 2016 October; 13(4):e23636. doi: 10.5812/iranjradiol.23636.

Published online 2016 June 25. **Research Article**

# Calcification in Globus Pallidus and Putamen of Multiple Sclerosis Patients Versus Healthy Subjects Using Quantitative Susceptibility Mapping

Muhammad Arshad Javid,[1,*] M Afzal Khan,[2] Naima Amin,[3] and Azeem Nabi[4]

[1]Department of Basic Sciences (Physics), University of Engineering and Technology, Taxila, Pakistan
[2]Department of Physics, Islamia University of Bahawalpur, Bahawalpur, Pakistan
[3]Department of Physics, Comsats University, Lahore, Pakistan
[4]Department of Physics, University of Gujrat, Gujrat, Pakistan

[*]*Corresponding author*: Muhammad Arshad Javid, Department of Basic Sciences (Physics), University of Engineering and Technology, Taxila, Pakistan. Tel: +92-03336345363, Fax: +92-0519047873, E-mail: arshadrahictn@gmail.com

**Received** 2014 September 15; **Revised** 2015 May 28; **Accepted** 2015 July 14.

## Abstract

**Background:** Calcification has been well reported in basal ganglia and it grows rapidly in globus pallidus (GP) followed by putamen (PUT) and caudate nucleus because of their high metabolic rate and displays high susceptibility effects. Therefore, the current study focused on magnetic susceptibility effect of calcium content in normal and diseased tissue due to metabolic changes.
**Objectives:** To evaluate calcium content in GP and PUT structures of multiple sclerosis (MS) patients versus healthy subjects using quantitative susceptibility mapping.
**Patients and Methods:** We compared 10 MS patients with mean age of 48.3 years (standard deviation [SD]=11.89) with 10 healthy subjects with mean age of 39.6 years (SD=11.52). Scanning of subjects was performed with high resolution ($0.5 \times 0.5 \times 2$ mm$^3$) using susceptibility weighted imaging sequence on 3 Tesla (Trio-Siemens, Erlangen, Germany). Data was processed in homemade SPIN software to produce susceptibility mapping. Threshold was set in healthy subjects to detect calcium content in PUT and GP structures.
**Results:** Magnetic susceptibility($x$) of calcium content was assessed by number of pixels induced by GP and PUT in MS patients as well as healthy subjects. Two sample t-test was used to assess the difference between susceptibilities of GP and PUT of MS patients ($P = 0.06$, $P > 0.05$). Susceptibilities of GP and PUT also showed $P = 0.3$ in healthy subjects. One way analysis of variance was used to assess the difference of susceptibilities in four variables of both populations. Insignificant results ($P = 0.7$, $P > 0.05$) were found among four variables. There was no statistically significant difference between magnetic susceptibilities of both populations.
**Conclusion:** Statistical analysis of susceptibilities of MS patients versus healthy subjects found no excess deposition of calcium content in deep gray matter of MS patients. Calcification may not be considered as a biomarker of prognosis in MS.

*Keywords:* Basal Ganglia Calcification, Brain Diseases, Multiple Sclerosis

## 1. Background

Calcification has been associated with several intracranial pathologies including tumor, cerebrovascular diseases, congenital conditions, trauma and metabolic disorders (1). Siglin et al. reported that calcification in basal ganglia is associated to hyperparathyroidism (2). It is a morphological feature of the pineal gland and is considered a marker of secretory activity of the gland and degeneration in multiple sclerosis (MS) (3). Dolores et al. demonstrated that calcification in basal ganglia has been a subcortical pattern of neuropsychological dysfunction and behavioral changes (4). The association between basal ganglia calcification and psychiatric abnormality has been found in schizophrenia (5). Idiopathic basal ganglia calcification has been reported in neuropsychiatric abnormalities, disturbances of movement, normal calcium and phosphorus metabolism (6).

Besides the iron content in brain, there are other few diamagnetic elements such as calcium, magnesium, potassium, phosphorus, aluminum and copper, which mitigate the effect of iron on susceptibility weighted imaging (SWI) (7). These diamagnetic contents deposit in the brain and oppose the blood flow and cause neural tissue injury (8). Generally, calcification can be identified using computed tomography (CT) (9, 10). However, identification of calcification by magnetic resonance imaging (MRI) is not well exquisite due to the variability of signals on conventional T1-weighted (T1-W) or T2-W images (11). Therefore, quantitative susceptibility mapping (QSM) determines magnetic susceptibility of underlying tissue from measurements of magnetic field perturbation (12). Consequently, susceptibility mapping corresponds to hypointense areas and displays diamagnetic susceptibility variations. Furthermore, QSM provides fast, convenient and effective physiological and pathophysiological information by quantifying iron and calcification in a tissue in degenerative diseases such as MS, Parkinson's disease and Alzheimer's disease (12-16). Hitherto, calcification has been reported little in patients with MS using QSM.

## 2. Objectives

This article aimed to evaluate calcium content in putamen (PUT) and globus pallidus (GP) structures in MS patients using QSM, so that pathological information may be predicted based on calcification.

## 3. Patients and Methods

### 3.1. Subjects

This study was approved by the local ethics committee and an informed consent was obtained from each individual. We collected data of ten MS patients aged 48.3 years, (standard deviation[SD]=11.89) with clinically definite relapsing-remitting MS and disease duration between 0 to 3 years and ten healthy subjects with mean age of 39.6 years, (SD=11.52). Both healthy subjects and MS patients were enrolled in Harper University hospital in MR research facility center, Detroit, MI, USA under project to compare the flow quantification in MS patients versus healthy subjects.

### 3.2. Data Acquisition

Magnetic resonance images of high resolution were acquired at 3 Tesla (Trio-Siemens, Erlangen, Germany) with an in-plane resolution of ($0.5 \times 0.5 \times 2$ mm$^3$) using three dimensional (3D) SWI sequence, echo time (TE) = 20 ms, repetition time (TR) = 30 ms, matrix size = $512 \times 384$, bandwidth pixel = 100, flip angle (F.A) =15°.

### 3.3. Statistical Analysis

Calcium content in GP and PUT structures was assessed using the value of magnetic susceptibilities in each region of interest. Statistical analysis was performed using OrgionPro.8 software (china, www.origionLab.com). $P \leq 0.05$ was considered as statistically significant. We performed two sample t-test to assess the difference in susceptibility between MS patients and healthy subjects. The susceptibilities of GP and PUT showed consistency such as GP ($P = 0.06$) and putamen ($P = 0.2$) in MS patients and healthy subjects as shown in Figure 1. Furthermore, Kolmogorov- Smirnov test was performed to assess normal distribution of susceptibility data. One way analysis of variance (ANOVA) was performed to assess the difference of susceptibilities in four variables of both populations. There was no significant difference ($P = 0.7, P > 0.05$) among four variables. The susceptibilities of GP and PUT showed insignificant results ($P > 0.05$) in MS patients compared to healthy subjects. Statistically results presented no difference in magnetic susceptibilities of both populations.

### 3.4. Data Processing

SPIN (signal processing in nuclear magnetic resonance [NMR]) homemade software (MRI institute for biomedical research, Detroit, MI, USA) is based on visual $C^{++}$ that can measure structural measurements in 3D, iron content, microhemorrhage quantification and calcification (17, 18).

SPIN is also used to show the number of pixels, mean, SD, maximum intensity and minimum intensity within the regions of interest (ROI). GP and PUT regions were drawn manually by the author in SPIN based on their anatomical locations of deep gray matter of brain. GP and PUT were drawn on same slices and homogeneous regions were selected more than three slices. These two ROIs were double checked to evaluate the number of pixels with standard deviation in these two structures (17). A high pass filter of size ($64 \times 64$) was used to remove unnecessary background frequencies due to air or tissue interfaces (18). Threshold was estimated in PUT and GP in normal subjects on structures bilaterally, minus two times the SD. Threshold was calculated to detect calcium content in PUT (-51) and GP (-49) for 10 healthy subjects. Consequently, it was used as a reference to detect calcium content in GP and PUT of MS patients. Pixels intensity was captured at High Values in SPIN using positive threshold for iron content, which showed positive susceptibility ($X > 0$) known as a paramagnetic content or iron content. We did not concern to assess iron content during this study. We assessed only calcium content in GP and PUT of brain. Pixels were highlighted choosing "Low values" option in SPIN at specific negative threshold that were known as calcium content. Low values reflected the magnetic susceptibility of diamagnetic content (calcium) in selected regions, which were measured at defined negative axes ($X < 0$) of SPIN. Resultantly, calcium content displayed negative susceptibility on susceptibility mapping and values of calcium content were imported in excel sheet and saved automatically.

## 4. Results

To evaluate calcium content in GP and PUT structures, the pixel intensity in these ROIs were assessed in MS patients and healthy subjects. Total number of pixels induced by calcium content in GP were measured (ngms = 88) with ratio (0.09) for MS patients and total number of pixels induced by control subjects were measured (ngc = 499) with ratio (0.42). Total number of pixels for calcium content in PUT for MS patients and control subjects were measured (npms = 282) with ratio (0.19) and (npc = 442) with ratio (0.28), respectively. The pixel ratio was measured as the number of pixel produced by calcium content divided by total number of pixels in that region. Table 1 shows pixel

value and pixel ratio of calcium content in GP and PUT of brain in MS patients and healthy subjects. Calcium content being a hypointense (negative susceptibility opposite to iron content) was shown in Figure 1A and 1B in GP and PUT of MS patients on susceptibility mapping. Mean susceptibility of calcium content in GP structure of 10 MS patients was measured (X = -63.55, S.D = 11.52) and sum of susceptibility in left and right regions of GP was measured (X = -635.9). For 10 healthy subjects, the mean susceptibility of calcium content in GP was measured (X = -64.83, S.D = 12.2) and sum of susceptibilities was measured (X = -648.8).

Susceptibility of calcium content with SD measured in MS patients and healthy subjects are presented in Table 2.

Similarly, the mean susceptibility of calcium content in PUT structure of 10 MS patients was measured (X = -61, SD = 7.5) and sum of susceptibility was measured as (X = -612.2). Mean susceptibility with SD was measured (-63.2 $\pm$ 10.6) in 10 control subjects and total susceptibility was measured with value (X = -632.6). Distribution of calcium content in GP and PUT structures was assessed with mean values of susceptibilities in each region. Susceptibility of healthy subjects and MS patients are depicted in Figure 2 to show statistically significant results. The mean value of GP in control subjects showed an increasing trend compared to PUT, which depicted higher ratio of calcium content in GP. However, PUT showed subtle higher susceptibility values in MS patients. The reason for higher calcification of PUT is mentioned in reference 21. There was no statistically significant difference ($P > 0.5$) between both structures in MS patients under same MRI scanning protocol. Calcium content in PUT of MS and control subjects is shown in Table 3.

## 5. Discussion

Magnetic susceptibility in tissues provides a wealth of information such as accumulation of iron or calcium deposition in brain (1). Minerals such as calcium and iron induce different susceptibility effects that make phase images to be more sensitive in detecting deposition of minerals in brain (19). It has been well documented that iron is a paramagnetic in nature and produces a strong susceptibility effects, while calcium is a diamagnetic content and shows anti-iron susceptibility effect (1, 11-21).

To compare calcium content in MS patients versus control subjects, pixels intensity and susceptibilities of GP and PUT of brain were analyzed. The susceptibility of calcium content in GP and PUT of brain depicted negative phase behavior opposite to iron content on susceptibility mapping. Calcium content appeared hypointense on SW images due to its negative local phase shift (12, 20). Our study demonstrated the variability of pixel intensity in PUT and GP of brain due to variable concentrations of calcium in both populations. This variation in pixel intensity was reported by Zhu et al. in detection of intracranial calcification using SWI for healthy subjects (22, 23). Yamada et al. presented that calcification in basal ganglia has a phase shift with paramagnetic susceptibility using gradient echo phase imaging. He also differentiated susceptibility effects of calcium content among tissues as we observed negative susceptibility effect on susceptibility mapping for calcification (16). Similarly, Zhu et al. reported that adjacent tissues that contain ferritin, calcium and heme iron have different magnetic susceptibility (22). Harder et al. documented mineralization in deep gray matter structures of brain using SWI and compared the behavior of pixel intensity in PUT and GP (24). Gong et al. also presented that signal intensity changes on MRI are due to calcification in brain (25, 26). This study presented subtle variability of pixel intensity for calcification in GP and PUT in deep gray matter structures of brain due to various concentrations and proportion of calcium as reported in references (16, 22, 24).

Previous MR studies demonstrated that calcification starts from the caudate and PUT structures. It produces an ischemic injury and a variety of neurological disorders in brain due to abnormal incidence of calcium in tissues (19). Dehkarghani et al. documented that calcification occurred in the GP first in the aging brain (27). Cohen et al. reported that calcification is confined to GP in the brain. Literature survey demonstrated that calcification in pineal gland, choroid plexus and basal ganglia are associated with intracranial pathologies and aging effect (11). Harder et al. reported that mineralization increases with age (24). Cohen et al. reported that calcification in GP is found higher than other structures of basal ganglia and frequency of calcification increases with age of more than 40 years (7). In this study, calcium accumulation was found to be increased in both structures after 30 years of age. GP at age more than 30 years showed higher calcification either in MS patients or healthy subjects. Therefore, accumulation of calcium content in parenchyma at both structures showed equivalent tendency of susceptibility due to metabolic changes (28).

This study found that susceptibility mapping is more sensitive than conventional MRI to evaluate the amount of calcification in patients with MS. We made an effort to set threshold to evaluate calcification in PUT and GP structures of brain in MS patients that may be used easily by radiologists and medical physicists using MR phase images. This work may be helpful to find accumulation of calcification in neurodegenerative diseases using QSM.

Statistically analysis of susceptibilities of MS patients with healthy subjects showed no excess deposition of cal-

**Table 1.** Pixel Value of Calcium Content in Globus Pallidus and Putamen

| GP | | | | | | PUT | | | | | |
|---|---|---|---|---|---|---|---|---|---|---|---|
| $n_{gms}$ | N | $R_{ms}$ | $n_{gh}$ | N | $R_h$ | $n_{pms}$ | N | $R_{ms}$ | $n_{ph}$ | N | $R_h$ |
| 5 | 987 | 0.005 | 78 | 1445 | 0.054 | 41 | 1386 | 0.030 | 89 | 1572 | 0.057 |
| 4 | 1167 | 0.003 | 126 | 1369 | 0.092 | 5 | 1040 | 0.005 | 38 | 1713 | 0.022 |
| 3 | 1070 | 0.003 | 28 | 1353 | 0.021 | 8 | 1073 | 0.007 | 46 | 1582 | 0.029 |
| 3 | 1256 | 0.002 | 4 | 940 | 0.004 | 21 | 1330 | 0.016 | 9 | 1153 | 0.008 |
| 2 | 1195 | 0.002 | 20 | 882 | 0.023 | 45 | 1409 | 0.032 | 90 | 1631 | 0.055 |
| 20 | 870 | 0.023 | 35 | 1278 | 0.027 | 7 | 1195 | 0.006 | 30 | 1813 | 0.017 |
| 14 | 887 | 0.016 | 25 | 1273 | 0.020 | 33 | 1660 | 0.020 | 26 | 1304 | 0.020 |
| 23 | 949 | 0.024 | 26 | 1363 | 0.019 | 62 | 1524 | 0.041 | 13 | 1482 | 0.009 |
| 5 | 1032 | 0.005 | 96 | 1050 | 0.091 | 31 | 1648 | 0.019 | 42 | 1499 | 0.028 |
| 9 | 1256 | 0.007 | 61 | 1207 | 0.051 | 29 | 1429 | 0.020 | 59 | 1402 | 0.042 |

Abbreviations: GP, globus pallidus; PUT, putamen; $n_{gms,}$ number of pixels for calcium content in GP; N, total number of pixels in ROIs; $R_{ms}$, ratio between ngms or npms and N, ngh, number of pixel in globus pallidus for healthy subjects; $n_{pms}$, number of pixel in putamen for MS patients; $n_{ph}$, number of pixel in putamen for healthy subjects; $R_h$, pixel ratio for healthy subjects.

**Table 2.** X (ppb) of Globus Pallidus in Multiple Sclerosis Patients and Healthy Subjects at Threshold (-49)

| Age (MS) Years | X (Mean) MS (ppb) | SD | X (Total) (ppb) | X (Mean) H (ppb) | SD | X (Total) (ppb) |
|---|---|---|---|---|---|---|
| 40 | -54 | 3.7 | -197 | -62.81 | 12.1 | -4899 |
| 17 | -48 | 5.0 | -240 | -56.75 | 17.4 | -9077 |
| 36 | -67 | 6.5 | -438 | -59.71 | 13.1 | -1672 |
| 41 | -55 | 4.3 | -238 | -65.75 | 6.8 | -227 |
| 33 | -58 | 3.0 | -174 | -68.6 | 13.5 | -1315 |
| 45 | -84 | 5.7 | -2159 | -62.44 | 21.6 | -2401 |
| 46 | -56.5 | 6.6 | -1269 | -59.35 | 9.6 | -1561 |
| 33 | -67.1 | 9.3 | -627 | -74.11 | 8.7 | -1543 |
| 33 | -61.4 | 8.5 | -520 | -66.73 | 13.1 | -7115 |
| 52 | -64.9 | 9.3 | -604 | -72.04 | 6.1 | -4071 |

Abbreviations: MS, multiple sclerosis; H, healthy; SD, standard deviation; X (ppb), susceptibility of calcium content in parts per billion.

**Table 3.** X (ppb) of Putamen in Multiple Sclerosis Patients and Healthy Subjects at Threshold (-51)

| Age (MS) Years | X (Mean) MS (ppb) | SD | X (Total) (ppb) | X (Mean) H (ppb) | SD | X (Total) (ppb) |
|---|---|---|---|---|---|---|
| 40 | -63.0 | 8.9 | -2519 | -63.73 | 13.5 | -2613 |
| 17 | -56.6 | 4.3 | -962 | -61.37 | 9.8 | -2946 |
| 36 | -61.1 | 6.0 | -2201 | -64.63 | 8.7 | -2197 |
| 41 | -61.5 | 6.6 | -2521 | -55.67 | 4.1 | -1614 |
| 33 | -58.4 | 5.2 | -1927 | -63.16 | 8.7 | -2842 |
| 45 | -57.0 | 4.1 | -2565 | -67.30 | 15.9 | -3163 |
| 46 | -73.9 | 17.0 | -3401 | -67.23 | 14.1 | -3630 |
| 33 | -61.1 | 8.7 | -2017 | -61.08 | 6.6 | -3298 |
| 33 | -59.8 | 6.0 | -1974 | -64.88 | 14.8 | -4087 |
| 52 | -60.3 | 8.5 | -3134 | -63.19 | 10.2 | -4233 |

Abbreviations: MS, multiple sclerosis; H, healthy; SD, standard deviation; X (ppb), susceptibility of calcium content in parts per billion.

cium content in deep gray matter of MS patients. Calcification may not be considered a biomarker of prognosis in

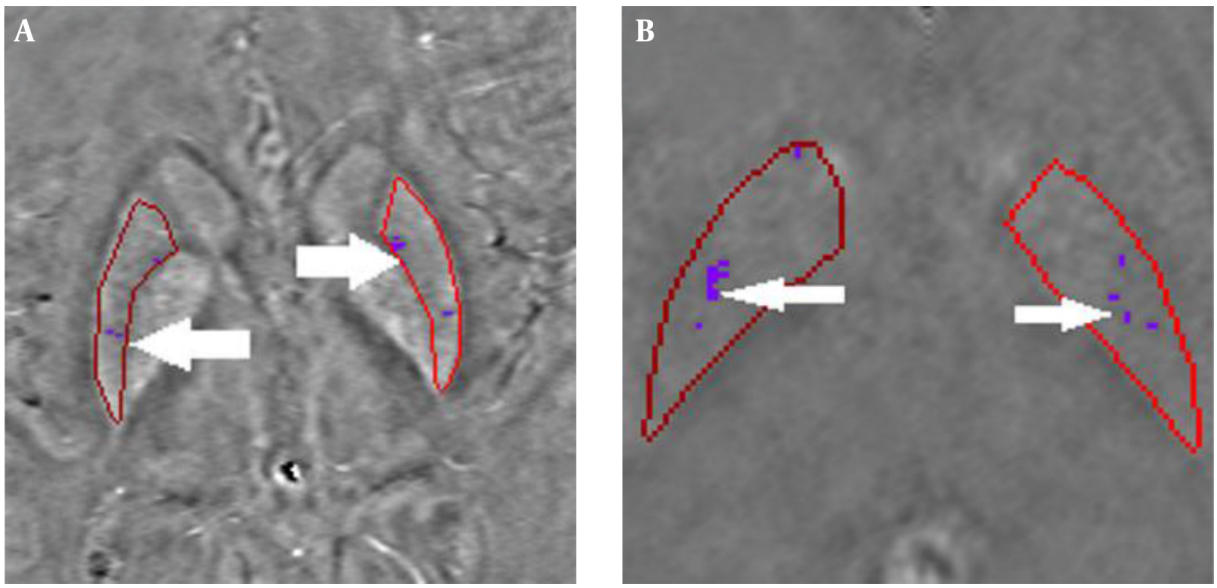


**Figure 1.** Quantitative susceptibility mapping showing calcium content in a 33-year old female; A, Calcium content in putamen at threshold (-51); B, Calcium content in globus pallidus at threshold (-49)

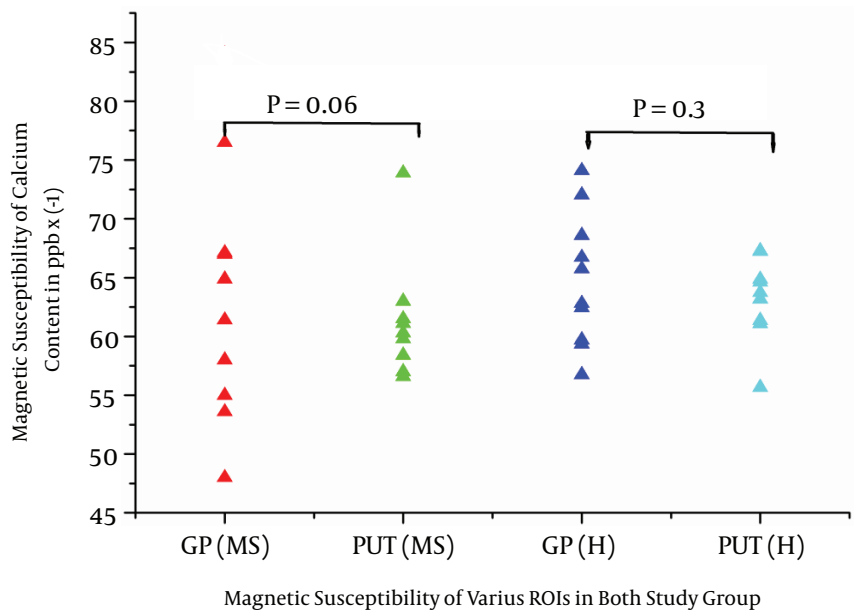


**Figure 2.** Magnetic susceptibility of various regions of interest (ROIs) in multiple sclerosis (MS) patients versus healthy (H) subjects (GP, globus pallidus; PUT, putamen)

MS.

## Supplementary Material

Supplementary material(s) is available here.

## Acknowledgments

We are thankful to Dr. E.M Haacke and Dr. Neelavalli Jaladhar who helped us to perform this project in institute of biomedical research, Detroit, MI, USA.

## Footnote

**Authors' Contribution:** Muhammad Arshad Javid worked on this project in the USA; M Afzal Khan was supervisor of this project and helped in data analysis; Naima Amin worked in data analysis. Azeem Nabi worked on literature survey.

## References


1. Wu Z, Mittal S, Kish K, Yu Y, Hu J, Haacke EM. Identification of calcification with MRI using susceptibility-weighted imaging: a case study. *J Magn Reson Imaging.* 2009;**29**(1):177–82. doi: 10.1002/jmri.21617. [PubMed: 19097156].
2. Siglin IS, Eaton LM. Symmetric cerebral calcification which followed post-operative parathyroid insufficiency; report of a case. *J Clin Endocrinol Metab.* 1947;**7**(6):433–7. doi: 10.1210/jcem-7-6-433. [PubMed: 20253394].
3. Zimmerman RA, Bilaniuk LT. Age-related incidence of pineal calcification detected by computed tomography. *Radiology.* 1982;**142**(3):659–62. doi: 10.1148/radiology.142.3.7063680. [PubMed: 7063680].
4. Lopez-Villegas D, Kulisevsky J, Deus J, Junque C, Pujol J, Guardia E, et al. Neuropsychological alterations in patients with computed tomography-detected basal ganglia calcification. *Arch Neurol.* 1996;**53**(3):251–6. [PubMed: 8651878].
5. Francis A, Freeman H. Psychiatric abnormality and brain calcification over four generations. *J Nerv Ment Dis.* 1984;**172**(3):166–70. [PubMed: 6142086].
6. Trautner RJ, Cummings JL, Read SL, Benson DF. Idiopathic basal ganglia calcification and organic mood disorder. *Am J Psychiatry.* 1988;**145**(3):350–3. doi: 10.1176/ajp.145.3.350. [PubMed: 3344850].
7. Cohen CR, Duchesneau PM, Weinstein MA. Calcification of the basal ganglia as visualized by computed tomography. *Radiology.* 1980;**134**(1):97–9. doi: 10.1148/radiology.134.1.7350641. [PubMed: 7350641].
8. Haacke EM, Mittal S, Wu Z, Neelavalli J, Cheng YC. Susceptibility-weighted imaging: technical aspects and clinical applications, part 1. *AJNR Am J Neuroradiol.* 2009;**30**(1):19–30. doi: 10.3174/ajnr.A1400. [PubMed: 19039041].
9. Makariou E, Athos DP. Intracranial calcification; applied radiology. 2009 :48–60.
10. Kiroglu Y, Calli C, Karabulut N, Oncel C. Intracranial calcifications on CT. *Diagn Interv Radiol.* 2010;**16**(4):263–9. doi: 10.4261/1305-3825.DIR.2626-09.1. [PubMed: 20027545].
11. Deistung A, Schweser F, Wiestler B, Abello M, Roethke M, Sahm F, et al. Quantitative susceptibility mapping differentiates between blood depositions and calcifications in patients with glioblastoma. *PLoS One.* 2013;**8**(3):ee57924. doi: 10.1371/journal.pone.0057924. [PubMed: 23555565].
12. Schweser F, Sommer K, Deistung A, Reichenbach JR. Quantitative susceptibility mapping for investigating subtle susceptibility variations in the human brain. *Neuroimage.* 2012;**62**(3):2083–100. doi: 10.1016/j.neuroimage.2012.05.067. [PubMed: 22659482].
13. Deistung A, Mentzel HJ, Rauscher A, Witoszynskyj S, Kaiser WA, Reichenbach JR. Demonstration of paramagnetic and diamagnetic cerebral lesions by using susceptibility weighted phase imaging (SWI). *Z Med Phys.* 2006;**16**(4):261–7. [PubMed: 17216751].
14. Schafer A, Forstmann BU, Neumann J, Wharton S, Mietke A, Bowtell R, et al. Direct visualization of the subthalamic nucleus and its iron distribution using high-resolution susceptibility mapping. *Hum Brain Mapp.* 2012;**33**(12):2831–42. doi: 10.1002/hbm.21404. [PubMed: 21932259].
15. Mittal S, Wu Z, Neelavalli J, Haacke EM. Susceptibility-weighted imaging: technical aspects and clinical applications, part 2. *AJNR Am J Neuroradiol.* 2009;**30**(2):232–52. doi: 10.3174/ajnr.A1461. [PubMed: 19131406].
16. Yamada N, Imakita S, Sakuma T, Takamiya M. Intracranial calcification on gradient-echo phase image: depiction of diamagnetic susceptibility. *Radiology.* 1996;**198**(1):171–8. doi: 10.1148/radiology.198.1.8539373. [PubMed: 8539373].
17. Haacke EM, Ayaz M, Khan A, Manova ES, Krishnamurthy B, Gollapalli L, et al. Establishing a baseline phase behavior in magnetic resonance imaging to determine normal vs. abnormal iron content in the brain. *J Magn Reson Imaging.* 2007;**26**(2):256–64. doi: 10.1002/jmri.22987. [PubMed: 17654738].
18. Neelavalli J, Cheng YC, Jiang J, Haacke EM. Removing background phase variations in susceptibility-weighted imaging using a fast, forward-field calculation. *J Magn Reson Imaging.* 2009;**29**(4):937–48. doi: 10.1002/jmri.21693. [PubMed: 19306433].
19. Fatemi-Ardekani A, Boylan C, Noseworthy MD. Identification of breast calcification using magnetic resonance imaging. *Med Phys.* 2009;**36**(12):5429–36. doi: 10.1118/1.3250860. [PubMed: 20095255].
20. Gupta RK, Rao SB, Jain R, Pal L, Kumar R, Venkatesh SK, et al. Differentiation of calcification from chronic hemorrhage with corrected gradient echo phase imaging. *J Comput Assist Tomogr.* 2001;**25**(5):698–704. [PubMed: 11584228].
21. Thomas B, Somasundaram S, Thamburaj K, Kesavadas C, Gupta AK, Bodhey NK, et al. Clinical applications of susceptibility weighted MR imaging of the brain - a pictorial review. *Neuroradiology.* 2008;**50**(2):105–16. doi: 10.1007/s00234-007-0316-z. [PubMed: 17929005].
22. Zhu WZ, Qi JP, Zhan CJ, Shu HG, Zhang L, Wang CY, et al. Magnetic resonance susceptibility weighted imaging in detecting intracranial calcification and hemorrhage. *Chin Med J (Engl).* 2008;**121**(20):2021–5. [PubMed: 19080268].
23. Schenker C, Meier D, Wichmann W, Boesiger P, Valavanis A. Age distribution and iron dependency of the T2 relaxation time in the globus pallidus and putamen. *Neuroradiology.* 1993;**35**(2):119–24. [PubMed: 8433786].
24. Harder SL, Hopp KM, Ward H, Neglio H, Gitlin J, Kido D. Mineralization of the deep gray matter with age: a retrospective review with susceptibility-weighted MR imaging. *AJNR Am J Neuroradiol.* 2008;**29**(1):176–83. doi: 10.3174/ajnr.A0770. [PubMed: 17989376].
25. Xiangyang G, Senhua L, Rongfen L, Xiang H, Xiaoya G, Fengfeng X. Experimental study of MRI signal changes of calcification. *Chinese J Radiol.* 1999;**33**(10):708–12.
26. Gong X, Li S, Li R. MRI signal variances of intracranial calcifications. *Chin J Radiol.* 1999;**33**(10):751–4.
27. Dehkharghani S, Dillon WP, Bryant SO, Fischbein NJ. Unilateral calcification of the caudate and putamen: association with underlying developmental venous anomaly. *AJNR Am J Neuroradiol.* 2010;**31**(10):1848–52. doi: 10.3174/ajnr.A2199. [PubMed: 20634305].
28. Takashima S, Becker LE. Basal ganglia calcification in Down's syndrome. *J Neurol Neurosurg Psychiatry.* 1985;**48**(1):61–4. [PubMed: 3156213].